N. NDE Inspection of Resistance Spot Welds in Automotive Structures Using an Ultrasonic Phased Array

Principal Investigator: Deborah Hopkins
Lawrence Berkeley National Laboratory
1 Cyclotron Road, MS 46A-1123, Berkeley, CA 94720
(510) 486-4922; fax: (510) 486-4711; e-mail: dlhopkins@lbl.gov

Technology Area Development Manager: Joseph Carpenter
(202) 586-1022; fax: (202) 586-1600; e-mail: joseph.carpenter@ee.doe.gov
Field Technical Manager: Philip S. Sklad
(865) 574-5069; fax: (865) 576-4963; e-mail: skladps@ornl.gov

Participants
U.S. Automotive Materials Partnership NDE of Welded Metals Steering Committee
Frédéric Reverdy, Ph.D., Lawrence Berkeley National Laboratory
Daniel Türler, M.S., Lawrence Berkeley National Laboratory
William B. Davis, M.S., Lawrence Berkeley National Laboratory

---

Contractor: Lawrence Berkeley National Laboratory
Contract No.: DE-AC03-765F0095

Objective

- Develop a cost-effective ultrasonic phased-array system that is sufficiently fast, accurate, and robust in manufacturing environments to be suitable for inspection of spot welds in automotive components.

Approach

- Develop a spot-weld inspection system that can be used by operators with minimal training by using state-of-the-art ultrasonic phased-array technology. The multielement probe allows the ultrasonic energy to be focused at the interface between the welded sheets and electronically scanned through the weld.
- Design a miniature mechanical scanner that will allow scanning in the direction perpendicular to the electronic scan to produce two-dimensional images of the weld. The portable system allows more than 3000 signals to be acquired in less than 4 s.
- Develop signal processing and image analysis software to distinguish satisfactory, undersized, and defective welds and provide dimensional analysis of the weld in a few seconds.
- Minimize the footprint of the probe assembly to ensure access to welds on complex components.
- Design an integrated probe housing that meets the size constraints while allowing mechanical scanning over a travel distance of 16 mm. The housing will also maintain the probe in water and must have an outer membrane that provides acoustic coupling to the part under inspection.
- Conduct plant trials to demonstrate the system's ability to characterize welds with sufficient accuracy and repeatability and to demonstrate that the integrated probe housing is rugged enough for use in a production facility.

Accomplishments

- Evaluated the performance and limitations of existing ultrasonic phased-array systems.
- Conducted a series of laboratory experiments to evaluate the performance of 5-, 10-, and 17-MHz phased-array probes for characterization of spot welds in galvanized steel.
- Developed signal-processing algorithms to distinguish between satisfactory, undersized, and defective welds.
- Developed image-processing algorithms that allow dimensional analysis of welds.
- Demonstrated the ability to acquire more than 3000 signals per weld and analyze the resulting data in a few seconds to render an estimate of weld quality.
- Demonstrated good correlation between ultrasonic measurements, measurements of weld buttons on peeled samples, and metallographic images of cross sections through welds.
- Designed a probe housing that maintains the probe in water, contains a miniature mechanical system that allows linear translation of the probe, and provides an outer membrane that confines the water column while also providing acoustic coupling to the part under inspection.

Future Direction

- Conduct laboratory experiments and plant trials to demonstrate the ability of phased-array systems to inspect spot welds with sufficient accuracy and repeatability for the full range of materials and joint configurations used in production.
- Conduct laboratory experiments to determine the concept feasibility of using ultrasonic phased arrays to inspect welds in aluminum and high-strength steel.
- Develop automated classifiers to determine weld dimensions and identify defective welds including cold welds.
- Identify and test coupling techniques that will allow existing probes to be used outside of a water tank.
- Develop a user interface in conjunction with end users to ensure ease of use and reporting of data in the most useful format for inspectors, welding engineers, and plant managers.
- Develop a fully integrated prototype system suitable for deployment and testing in a manufacturing plant.
- Perform large-scale testing and measurement system analysis.

Introduction

Development of nondestructive evaluation (NDE) techniques has been identified in both industry and government forums as an enabling technology for greater use of advanced and light-weight materials in the automotive industry. Reducing vehicle weight improves fuel efficiency and reduces emissions, and recent studies have demonstrated cost savings that derive from finding defects early in the production process and reducing waste compared to destructive testing. One of the critical technical challenges in introducing light-weight materials is developing joining technologies and inspection strategies suitable for mass production. NDE methods to assure product quality are essential for industry and consumer acceptance of new materials and manufacturing methods.

At present, the most common methods for inspecting spot welds in automotive manufacturing are pry checks and physical teardown, during which spot-welded joints are pried apart; the resulting weld buttons are visually inspected or measured with calipers. Although these methods have been used successfully for decades, destructive weld testing has several drawbacks including high costs associated with scrapped material, ergonomic injuries, and the time lag between the onset and identification of problems. In addition, pry tests and teardowns do not allow plant managers and engineers to easily collect inspection data that would allow them to identify trends and potential problems. Furthermore, these inspection techniques are not viable options for lightweight and high-strength materials. Composite structures with adhesive-bonded joints

cannot be pry checked, and aluminum is relatively expensive and more difficult to rework than steel making pry checks and teardown cost prohibitive. Welds in high-strength steel are often too strong to be pry checked or torn down, and satisfactory welds sometimes fail interfacially rather than by pulling a weld button, making it difficult for inspectors to distinguish between satisfactory and defective welds.

Advances in sensors, computing, communication, and engineering technologies have all played a role in advancing the development of NDE methods with promising automotive applications. For example, ultrasonic phased-array systems have been available since the mid-1970s, but they were prohibitively expensive. In the past decade, prices have dropped dramatically, and increased competition promises additional price reductions in the future. A recent breakthrough is the availability of portable systems that are particularly attractive for use in production environments.

Lawrence Berkely National Laboratory (LBNL) previously evaluated the adequacy of conventional, commercially available ultrasonic systems for the inspection of spot welds. Although these systems are widely used in European automotive plants, they have not gained widespread acceptance in the United States for reasons that include their dependence on trained operators to set system variables and the need to change probes frequently because of the wide range of materials and sheet thicknesses used in production vehicles. An important goal of the current project is to develop a system that is much easier to use. Plant managers also emphasize the need for intuitive user interfaces and summary reports that can be customized for welding engineers and other plant personnel.

To best advance the adoption of lightweight materials while also serving the needs of the auto industry, the current project team has adopted a strategy that strives to develop platforms that add value immediately, minimize barriers to incorporating emerging technologies at a later date, and that are as modular as possible so that they can be easily modified or adapted for new applications. Consistent with that model, the current work is focused on development of a prototype spot-weld inspection platform that integrates the best available ultrasonic phased-array technology with custom-designed signal processing and analysis software, and hardware that will allow the system to be tested and implemented in manufacturing plants as a portable stand-alone unit.

Ultrasonic Phased-Array Technology

The only commercial spot-weld inspection systems available today use conventional high-frequency, single-crystal, ultrasonic probes working in pulse-echo mode. The output from these mono-probes is a single signal that is an integrated response over an area that depends on the diameter of the probe. Different probes must be used for different sized welds. In contrast, a phased array is composed of many piezoelectric elements that are individually excited by electronic pulses at programmed delay times. As a result, phased arrays have several advantages over conventional ultrasonic probes that derive from the ability to dynamically control the acoustic beam transmitted into the structure under examination. An electronic delay can be applied separately to each electronic channel when emitting and receiving the signal. These delay laws permit constructive and destructive interference of the acoustic wavefront transmitted into the structure, allowing predefined ultrasonic beams to be formed. The acoustic energy can be focused, and delay laws can be used to steer the acoustic beam. Electronic scanning is accomplished by firing successive groups of elements in the array.

Instead of assessing weld quality based on a single signal, as is the case with mono-probes, phased arrays allow thousands of signals to be obtained for individual welds in a few seconds. The ability to perform complex scanning of the acoustic beam through the weld allows greater accuracy in sizing weld nuggets, while also improving the flaw characterization capability. These attributes of phased-array probes allow us to measure the weld-nugget diameter, locate defects, and identify mis-shapen and burnt welds. In addition, the same probe can be used to inspect different sized welds and welds in sheets with different thicknesses. It is also possible to electronically compensate for misalignment of the probe with respect to the sample.

Previous Work

Initial experiments were conducted using an R/D Tech ultrasonic phased-array system loaned to LBNL by the Ford Motor Company. The system consists of an electronic controller, a linear 5-MHz probe, and a data acquisition system. The system

was used to perform laboratory experiments designed to evaluate the performance of existing hardware, determine the optimal probe configuration, and to develop signal-processing and weld-classification algorithms.

An open question at the beginning of the project was the adequacy of the 5-MHz probe for the full range of materials and sheet thicknesses currently used in production. Phased-array probes are now available up to a frequency of about 20 MHz. In general, relatively high-frequency probes provide better spatial resolution than lower frequency probes, but are more expensive.

The results of the experiments conducted with the 5-MHz probe demonstrated that a central frequency of 5 MHz is too low to inspect welds in the thinnest metal sheets used in the automotive industry (thinner than 1 mm). Therefore, a new suite of experiments was carried out with leased probes with central frequencies of 10 and 17 MHz. The 10-MHz probe was a 32-element linear probe with a 0.4-mm pitch (distance between two successive elements), and the 17-MHz was a 128-element focused probe with a focal distance of 12.5 mm and a pitch of 0.28 mm. The distance between the probe and samples was held constant at 12.5 mm for all experiments to allow the same focal law to be used. The test specimens were spot-welded strips made from 1.4-mm-thick galvanized mild-steel sheet metal. Several hundred welds were inspected. Analysis of the resulting data showed that the focused 17-Mhz probe was the best choice for being able to inspect welds across the full range of sheet thicknesses used in production.

These initial experiments were performed in a water tank or using a confined water column with coupling gel between the probe and the sample. As described below, to allow measurements to be made in a production environment, a self-contained probe housing has been designed that maintains the probe in water while also providing acoustic coupling to the part under inspection.

Phased-Array Inspection Strategy

For all experiments performed to date, electronic scanning and focusing laws were combined to inspect the spot welds. The acoustic energy is focused at the interface between the two sheets by applying symmetrical delay laws to the elements (see Figure 1). The results presented here were obtained using the 17-MHz focused probe described in the previous section. Unlike the 5- and 10-MHz probes that have flat elements, the 17-MHz probe has curved elements that focus the energy with a natural focal length of 12.5 mm. When used in conjunction with the delay laws described above that focus the energy from multiple elements, the acoustic beam at the interface between the welded sheets is a circular spot that is scanned across the weld. Using a portable phased-array controller, more than 3000 signals are recorded for each weld in approximately 4 s.

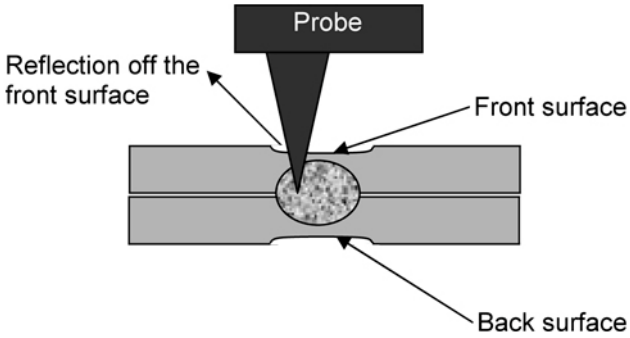

Figure 1. Schematic drawing illustrating focusing of the ultrasonic energy from several phased-array elements at the interface between two spot-welded sheets.

Scanning in one direction is performed by electronically translating the ultrasonic beam across the sample by firing a specified number of elements in sequence. For example, when eight elements are used at a time, the beam is electronically scanned across the weld in steps of one element; that is, elements one through eight are excited to generate the first signal, elements two through nine are excited to generate the second signal, and so forth. To obtain two-dimensional (2-D) images of the weld, the probe is mechanically translated across the weld in the direction perpendicular to the electronic scan.

As described above and illustrated in Figure 1, the acoustic energy generated by several adjacent elements in the probe is focused and transmitted into the test specimen. Some of the energy is reflected off the front surface as indicated in the diagram. In the welded region, the signals pass through both sheets and are reflected off the back surface. It is interesting to note that the metallurgical changes in the welded area do not cause a change in acoustic impedance large enough to create a noticeable

reflection at the boundary of the weld nugget. Outside the welded region, the signals are confined to the top sheet; that is, the acoustic waves are reflected back and forth in the upper sheet, and no energy is transferred into the lower sheet.

Signal Processing

The signals recorded while scanning through the weld are analyzed in the time and frequency domains. For a satisfactory weld, ultrasonic waves are transmitted through the weld nugget and reflected off the back surface of the lower sheet (see Figure 1). In contrast, for a cold weld, incomplete fusion at the interface between the two sheets results in partial reflection of the ultrasonic energy at the interface. This affects the periodicity of the train of echoes; that is, signals that are reflected at the interface have a shorter travel path than signals that propagate through the weld, resulting in echoes in the time domain that are closer together than echoes off the back surface.

In the frequency domain, the power spectrum captures the periodicity of the ultrasonic echoes in the time domain. Examples of the power spectra obtained from raw signals are shown in Figure 2 for the beam focused inside a satisfactory weld [(Figure 2(*a*)] and inside a cold weld [Figure 2(*b*)]. The power spectra were calculated using the data between the first backwall echo and the end of the signal. The relative magnitude of the peaks in the spectra is indicative of the amount of energy reflected at the interface. For a satisfactory weld, the ultrasonic wave propagates through the weld and reflects back and forth between the front and back surfaces resulting in a major echo [labeled 1 in Figures 2(*a*) and 2(*b*)] that corresponds to the travel path through both sheets. For a cold weld [Figure 2(*b*)], where most of the energy is reflected at the interface between the two sheets, the magnitude of echo 1 is smaller than the magnitude of echo 2, which corresponds to a travel path equal to twice the thickness of the upper sheet.

As an example of how this frequency information is used, processed images obtained for satisfactory, undersized, and defective welds are displayed in the first column of Figure 3. For each of the 3216 signals that comprise each image, the ratio of the first peak to the second peak in the power spectrum was calculated and then compared to a threshold that was used to create the binary images. White corresponds to high transmission into the lower sheet, while black indicates areas where there is complete or partial reflection off the interface between the two sheets.

The peak-ratio images allow satisfactory and undersized welds to be distinguished according to the size of the area where there is significant transmission of energy into the lower sheet. Although defective welds such as cold welds can result in a

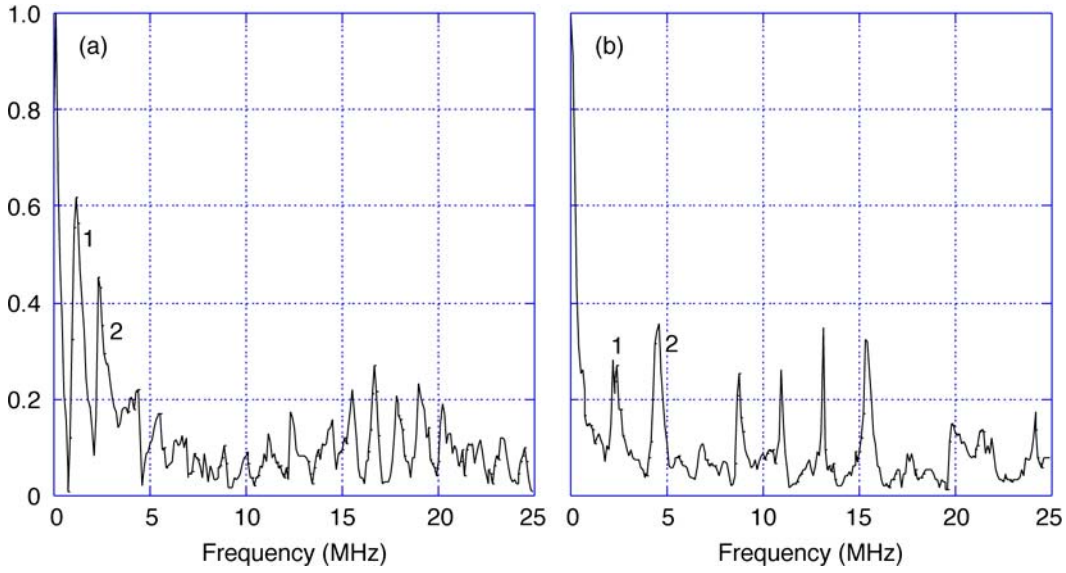

Figure 2. Fourier-based analysis showing the power spectra of individual signals obtained for a satisfactory weld (left-hand side) and a cold weld (right-hand side).

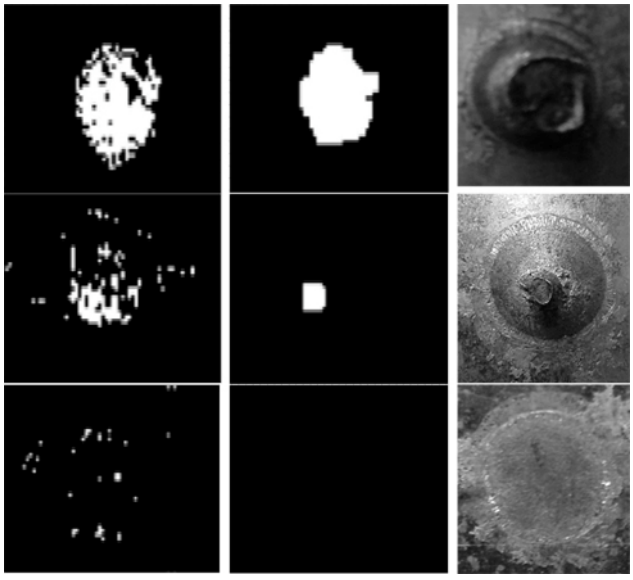

Figure 3. Binary images obtained by the Fourier peak-ratio method are displayed in the left-hand column for a satisfactory weld (top image), an undersized weld (middle image), and a defective weld (bottom image). The same images are displayed in the middle column after applying image-processing algorithms to obtain the contour of the largest zone of contiguous pixels with high transmission of acoustic energy across the interface between the two welded sheets. Photographs of the welds obtained after peeling the joints are shown in the right-hand column.

large area of ultrasonic transmission into the second sheet, the Fourier peak ratio indicates that the areas of high transmission are relatively sparse and dispersed compared to the well-defined and concentrated areas for the satisfactory and undersized welds. At present, the quality of the weld is assumed to be associated with the largest contiguous area of transmission. As described in the following sections, image-processing techniques are used to identify this area and separate it from the smaller transmission zones.

Connected Component Extraction

The first step in the process of determining whether individual pixels should be considered connected to or separate from the zone of interest is based on the operation of connected component extraction. Two points or pixels in a binary image are defined to be connected if a path can be found between them along which the characteristic function remains constant. In the examples presented here, the characteristic function is the value of the binary peak ratio. To implement this approach, it is necessary to define under what conditions two pixels are considered neighbors. For example, for four-point connectivity, only edge-adjacent pixels are considered neighbors (see Table 1). At present we are using eight-point connectivity: in this case, edge-adjacent and corner-adjacent pixels are considered neighbors.

The algorithm identifies and labels each distinct region contained within the image and associates an index to each area according to its size. The largest area is then extracted, and the smaller areas are discarded.

Table 1. Definitions of connectivity

	X
X	X
	X
X	X
O	O
X	X
	X
X	X
	X
Four-point connectivity	Eight-point connectivity

Morphological Filters of Erosion and Dilation

Morphological filters provide a wide range of operators that are commonly used for image processing. All of these operators are based on a few simple mathematical concepts from set theory, and they are particularly useful for the analysis of binary images. Common applications include edge detection, noise removal, image enhancement and image segmentation. The operations applied to the binary peak-ratio images are erosion and dilation. Erosion and dilation filters are used to add or remove pixels from the boundaries of features in order to smooth them or to join or separate portions of features. They are also used to remove isolated pixel noise from the image.

Dilation is the morphological transformation that combines two sets by using vector addition of

set elements. It is defined as the maximum of the sum of a local region of an image and a mask. The shape of the input mask (known as the structuring element, or SE) is generally chosen to emphasize or deemphasize elements in the image. Erosion is the opposite of dilation: erosion is used to smooth the boundaries between dark and light regions.

Ellipse Fitting

As discussed previously, during physical tear-down of automotive components, spot-welded joints are pried apart, and the resulting weld buttons are visually inspected or measured with calipers. To allow the results of the acoustic measurements to be compared to the size of the weld buttons, it is necessary to estimate weld dimensions from the peak-ratio images. Once the largest contiguous area of high acoustic transmission is identified and extracted, an ellipse is fit to the area as a means of estimating the size of the weld button.

Ellipse fitting is one of the classical problems in pattern recognition, and it has been the subject of considerable attention in the past 10 years because of its many applications. The technique described here is based on the method developed by M. Pilu (M. Pilu, A. Fitzgibbon, and R. Fisher "Ellipse-Specific Direct Least-Square Fitting," IEEE International Conference on Image Processing, Lausanne, September 1996).

The conic is represented as the zero set of an implicit second-order polynomial:

$$F(\mathbf{a},\mathbf{x}) = ax^2 + bxy + cy^2 + dx + ey + f \ ,$$

where **a** = [a, b, c, d, e, f] and **x** = [x^2, xy, y^2, x, y]. $F(a,x_i) = dist.$ is the "algebraic distance" between a point x_i and the conic $F(\mathbf{a},\mathbf{x}) = 0$. One way of fitting a conic is to minimize the algebraic distance over the set of **N** data points in the least-squares sense, that is:

$$dist. = \arg\ \min\left[\sum_{i=1}^{N} F(a, x_i)^2\right] \ .$$

The constraint $b^2 - 4ac = 0$ is imposed to yield elliptical solutions.

For our application, the objective is to find the edges of the largest area of ultrasonic transmission and to fit an ellipse to determine the dimensions of the major and minor axes. A simple gradient is applied to the image that has been processed using the connected-component-extraction algorithm and the morphological filters. Small anomalies in the interior of the image that occur because of small defects or a low signal-to-noise ratio are removed before applying the morphological filters. It is necessary to remove these points before applying the ellipse-fitting algorithm. Not doing so results in a low estimate of the ellipse dimensions. The boundary of the high-transmission zone is determined using the same connected-component-extraction algorithm that was used to extract the largest contiguous area (this algorithm can be improved by using a contour-tracking algorithm). The method is illustrated in Figure 4, which shows the best-fitting ellipse calculated for the processed binary peak-ratio image of a satisfactory weld.

The circumference of the satisfactory weld described above was measured to be 22 mm. The following approximation was used to calculate the circumference of the ellipse estimated using the ellipse-fitting algorithm:

$$P \approx \pi\left[3(a+b) - \sqrt{(3a+b)(a+3b)}\right] \ ,$$

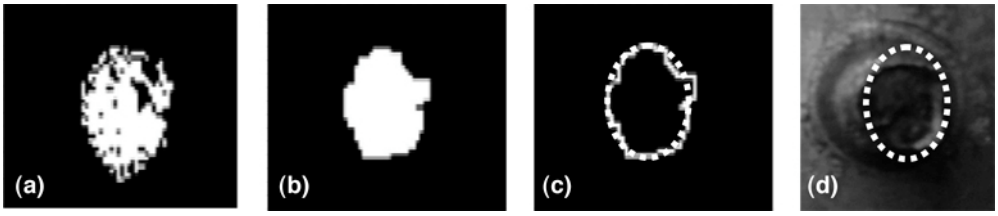

Figure 4. Binary image obtained by the Fourier peak-ratio method for a satisfactory weld (*a*), and the same image after applying image-processing techniques to obtain the contour of the zone of contiguous pixels with high transmission of acoustic energy across the interface between the two welded sheets (*b*). The dotted line in Figure (*c*) shows the ellipse fitted to the contour of the high-transmission zone. In Figure (*d*), the best-fitting ellipse is superposed on a photograph of the weld button obtained by peeling the joint.

where *a* and *b* are half the major and minor axes. The estimated perimeter of the fitted ellipse is 20.4 mm.

Metallography

While there is definitely a relationship between the size of the weld button obtained from peel tests and the size of the actual weld nugget, their dimensions are not exactly the same. To better understand this relationship, we compared the results of our signal-processing algorithms to images of cross sections through welds obtained using metallography. The samples were sectioned, polished, and etched to reveal the grain structure and the dimensions of the weld nugget. The following pictures show cross-sections through a satisfactory weld at different depths in the weld; the nugget is visible in the middle of the welded region where a characteristic dendritic grain structure is visible. The white squares denote the limit of the weld nugget as determined by visual inspection. The right-hand image shows the processed peak-ratio image obtained for this weld; the dotted lines indicate where the cross sections were made. These lines are superposed on the metallographic images to see how the algorithm performs.

Figure 5 shows the results of metallography compared to the output of the signal-processing algorithm for a satisfactory weld. The dotted lines indicate that the dimension of the processed image corresponds to the welded region visible in the metallographic image. Figure 6 shows a misshapen weld, in which there is no nugget formation in the center (see middle image in Figure 6). Although the welding parameters used in this case would normally produce a satisfactory weld, the metallographic images show that the weld nugget is actually C shaped with two separate nuggets. The processed image of the ultrasonic data also shows incomplete nugget formation and a C shape, although the small nugget on the right-hand side is not as clear on the processed peak-ratio image as it is in the metallographic images. This may be an effect of the morphological filters, which may have removed too many pixels during the erosion step. To explore this further, results obtained using erosion masks of different sizes will be compared to both metallographic images and weld buttons obtained from peel tests to determine the optimal mask size.

Probe Housing

A plant-deployable unit requires a housing for the ultrasonic probe that maintains the probe in water, contains a miniature mechanical system that allows linear translation of the probe, and that provides an outer membrane that confines the water column while also providing sufficient acoustic coupling to the part under inspection. Engineering the housing is extremely challenging because minimizing the footprint of the probe assembly is essential to ensure access to welds on complex components. The integrated probe assembly is also being

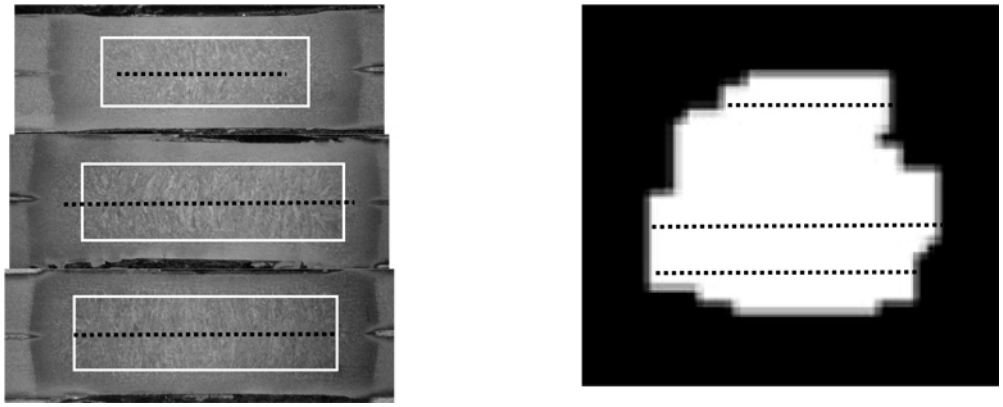

Figure 5. Metallographic images of a satisfactory weld obtained at three different depth levels in the weld (left-hand images) and the processed peak-ratio image obtained for the same weld (right-hand image). The white boxes in the metallographic images outline the boundary of the weld. The dotted lines in the right-hand image indicate the depths where cross sections of the weld were taken. These lines are superposed on the metallographic images to show the correspondence between the estimated weld diameter in the peak-ratio image and the apparent weld nugget in the metallographic images.

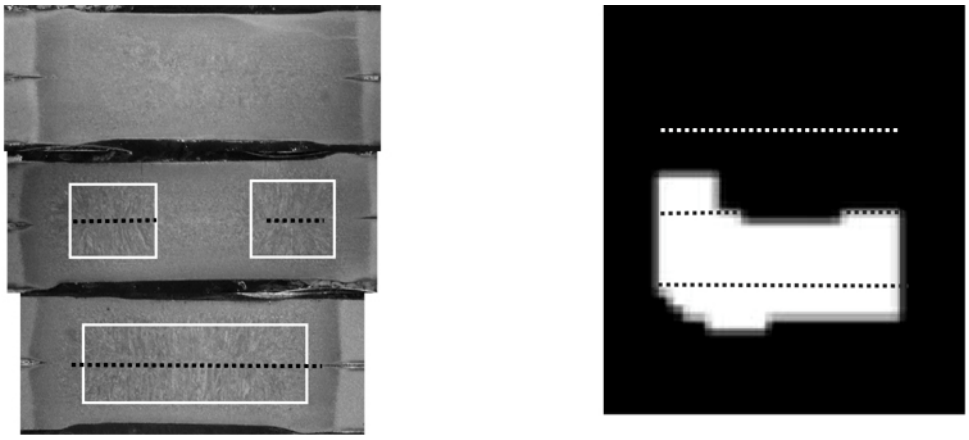

Figure 6. Metallographic images of a misshapen weld at three different depth levels in the weld (left-hand images) and processed peak-ratio image for the same weld (right-hand image). The white boxes in the metallographic images outline the boundary of the weld); note that there is no evidence of weld formation in the top image. The dotted lines in the right-hand image indicate the depths where cross sections of the weld were taken. These lines are superposed on the metallographic images to show the correspondence between the estimated weld diameter in the peak-ratio image and the apparent weld nugget in the metallographic images.

designed to allow for easy replacement of parts and troubleshooting.

For the current design, displayed in Figure 7, the overall footprint of the probe unit is 26 by 44 mm. Although the phased-array probe allows electronic scanning in one direction, mechanical scanning in the opposite direction is required to obtain 2-D images of the weld. A miniature mechanical system has been designed that allows a probe travel length of 16 mm. The small motor that will be used to drive the system has a nominal speed of 4800 rpm and is coupled to a 1:16 gearbox. The drive assembly is separated from the water column containing the probe by two slider plates and O-rings that form a watertight seal. The optimal material for the outer membrane is under investigation. Plant trials will be conducted to ensure that the integrated probe housing is rugged enough for use in a production facility.

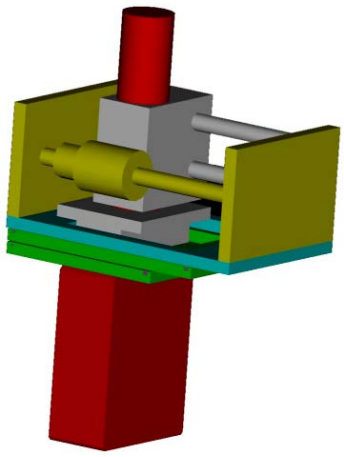

Figure 7. Mechanical drawing of the housing designed for the ultrasonic probe. The upper compartment houses the miniature mechanical system that will be used for linear translation of the probe. The lower compartment is a water chamber that contains the phased-array probe.

Conclusions

Work to date demonstrates that characterization of spot welds is possible using ultrasonic phased-array technology. Phased arrays have several advantages over mono-probes, including the ability to perform high-resolution scans that greatly increase detection and characterization capabilities. They are also less sensitive to probe placement and provide the ability to inspect a wide array of welds with a single probe. The remaining research challenge is to develop, test, and refine the techniques so that they are suitable for large-scale production facilities. Toward this end, a probe housing has been designed that will allow the system to be used in manufacturing plants. Work under way will also yield integrated real-time diagnostic tools that

operate at sufficient speed for assembly-line use. The remaining challenges include determination of resolution limits and the best diagnostic parameters for specific applications, and demonstration of robustness, accuracy, and cost-effectiveness under realistic operating conditions.

Presentations

1. C. Dasch, General Motors Corporation, "Strategic Review of Nondestructive Testing Technology," USCAR Materials Tech Team, July 21, 2004, Southfield, Michigan.
2. F. Reverdy, Lawrence Berkeley National Laboratory, "Inspection of Spot Welds Using a Portable Ultrasonic Phased-Array System," 31st Annual Review of Progress in Quantitative Nondestructive Evaluation, July 25–30, 2004, Colorado School of Mines, Golden, Colorado.
3. D. Hopkins, Lawrence Berkeley National Laboratory, "Development of an Ultrasonic Phased-Array System for Nondestructive Evaluation of Resistance Spot Welds," United States Automotive Materials Partnership (USAMP)—Automotive Materials Division (AMD) Offsite, December 2, 2004, Southfield, Michigan.